NASA/TM—1998-206981

Design and Operating Characteristics of High-Speed, Small-Bore, Angular-Contact Ball Bearings

Stanley I. Pinel
Pinel Engineering, Placentia, California

Hans R. Signer
Signer Technical Services, Fullerton, California

Erwin V. Zaretsky
NASA Lewis Research Center, Cleveland, Ohio

Prepared for the
Annual Meeting
sponsored by the Society of Tribologists and Lubrication Engineers
Detroit, Michigan, May 17–22, 1998

National Aeronautics and
Space Administration

Lewis Research Center

August 1998

Available from

NASA Center for Aerospace Information
7121 Standard Drive
Hanover, MD 21076
Price Code: A03

National Technical Information Service
5287 Port Royal Road
Springfield, VA 22100
Price Code: A03

DESIGN AND OPERATING CHARACTERISTICS OF HIGH-SPEED, SMALL-BORE, ANGULAR-CONTACT BALL BEARINGS

Stanley I. Pinel
Pinel Engineering
Placentia, California, U.S.A.

Hans R. Signer
Signer Technical Services
Fullerton, California U.S.A.

and

Erwin V. Zaretsky
National Aeronautics and Space Administration
Lewis Research Center
Cleveland, Ohio U.S.A

SUMMARY

The computer program SHABERTH was used to analyze 35-mm-bore, angular-contact ball bearings designed and manufactured for high-speed turbomachinery applications. Parametric tests of the bearings were conducted on a high-speed, high-temperature bearing tester and were compared with the computer predictions. Four bearing and cage designs were studied. The bearings were lubricated either by jet or through the split inner ring with and without outer-ring cooling. The predicted bearing life decreased with increasing speed because of increased operating contact stresses caused by changes in contact angle and centrifugal load. For thrust loads only, the difference in calculated life for the 24° and 30° contact-angle bearings was insignificant. However, for combined loading, the 24° contact-angle bearing gave longer life. For split-inner-ring bearings, optimal operating conditions were obtained with a 24° contact angle and an inner-ring, land-guided cage, using outer-ring cooling in conjunction with low lubricant flow rates. Lower temperature and power losses were obtained with a single-outer-ring, land-guided cage for the 24° contact-angle bearing having a relieved inner ring and partially relieved outer ring. Inner-ring temperatures were independent of lubrication mode and cage design. In comparison with measured values, reasonably good engineering correlation was obtained using the computer program SHABERTH for predicted bearing power loss and for inner- and outer-ring temperatures. The Parker formula for XCAV (used in SHABERTH, a measure of oil volume in the bearing cavity) may need to be refined to reflect bearing lubrication mode, cage design, and location of cage-controlling land.

INTRODUCTION

Aircraft turbine engines in the small class (0.45 to 4.5 kg/sec or 1 to 10 lb/sec total airflow) require rolling-element bearings to operate at temperatures to 218 °C (425 °F) and at speeds in excess of 2.5 M DN. (DN is defined as the speed of the shaft in revolutions per minute multiplied by the bearing bore in millimeters.) To achieve speeds of 3M DN with angular-contact ball bearings and cylindrical roller bearings, Zaretsky, Bamberger, and Signer (ref. 1) and Signer, Bamberger, and Zaretsky (ref. 2) proposed the concept of bearing thermal management as the proper technological approach to high-speed bearing operation. Under-ring-lubricated bearings were provided with outer-ring cooling. The basis of this concept was the recognition that total and flexible thermal control over all the bearing components was essential to achieving a reliable high-speed, highly loaded bearing. Research reported by Zaretsky, Bamberger, and Signer (ref. 1), Signer, Bamberger, and Zaretsky (ref. 2), and Bamberger, Zaretsky, and Signer (refs. 3 and 4) showed that bearings could be operated reliably for long periods at speeds to 3M DN with lubrication through annular passages extending radially through the bearing split inner ring and lands (underrace lubrication) and with outer-ring cooling.

Applying underrace lubrication to small-bore ball bearings is more difficult than applying it to larger bore sizes. Limited space is available for grooves and radial holes for supplying the lubricant under the inner ring. For a given DN value, centrifugal effects are more severe with small bearings because centrifugal force varies with the square of the speed where DN is proportional to speed. Heat generated per unit of surface area is much higher and heat removal is more difficult.

Schuller, Pinel, and Signer (refs. 5 to 10) performed parametric tests on AISI M–50, 35-mm-bore, angular-contact ball bearings. The bearings had a nominal, unmounted contact angle of 24° and either a single- or a double-outer-ring, land-guided cage. The investigation included lubrication by oil jets or through passages in the bearing inner ring. When inner-ring lubrication was used, the oil was channeled through axial grooves and radial holes in the bearing inner ring. In some tests, 50 percent of the oil supplied to the inner race was introduced into the bearing for lubrication, and 50 percent cooled the inner-ring exterior surfaces. In other tests, the distribution was 25 percent lubrication and 75 percent cooling. In selected tests, the bearing outer diameter was cooled with a constant oil flow of 1700 cm^3/min (0.45 gal/min) (ref. 11).

Test conditions included nominal shaft speeds from 30 000 to 72 000 rpm, (1.0 to 2.5 M DN), a radial load of 222 N (50 lbf), and/or a thrust load of 667 N (150 lbf). Lubricant flow to the bearing ranged from 0.3 to 1.9 ℓ/min (0.08 to 0.50 gal/min) at an inlet temperature of 121 °C (250 °F). All bearings were successfully run at speeds to 2.5 M DN.

The objective of the research reported herein was to extend the work of Schuller, Pinel, and Signer (refs. 5 to 10) to include the effects of bearing and cage design, shaft speed, lubricant flow rate, and outer-ring cooling on the operation of 35-mm-bore ball bearings.

APPARATUS, SPECIMENS, AND PROCEDURE

High-Speed Bearing Tester

A schematic drawing of the air-turbine-driven test machine is shown in figure 1 and was initially described by Pinel and Signer (ref. 12). The test rig consisted of a horizontally mounted shaft supported by two preloaded, angular-contact ball bearings. The test bearing was overhung and mounted in a separate housing that incorporated the hardware for lubrication, oil removal, thrust, radial load application, and instrumentation for cage speed measurement. The test bearing torque was measured with strain gages located near the end of an arm that prevented the housing from rotating. Thrust force was applied through the combination of a thrust needle bearing and a small roller support bearing to minimize test-housing restraint during torque measurements.

The test bearing can either be lubricated through the bearing inner ring and/or by lubricant jets on the nonloaded side of the inner race. For jet lubrication, the test bearing was lubricated by two jets on the nonloaded side of the inner ring. The jet outlets, located approximately 3 mm (0.12 in.) from the face of the bearing, were aimed at the inner raceway. In separate tests not reported herein, it was determined that a 20-m/sec (66-ft/sec) jet velocity provided the most efficient test bearing lubrication so this velocity was used in all the tests reported. (Miyakawa, Seki, and Yokoyama (ref. 13) reported a similar efficiency with a 20-m/sec (66-ft/sec) jet velocity over other

velocities.) Cooling oil was supplied to the outer ring by means of holes and grooves in the bearing housing, as shown in figure 1.

For inner-ring lubrication, oil was pumped by centrifugal force from the center of the hollow shaft through axial grooves in the test bearing bore and through a series of small radial holes, 0.762 mm (0.030 in.) in diameter, to the bearing inner race. Those axial grooves in the bearing bore that did not have radial holes allowed oil to flow under the ring for inner-ring cooling. To vary the distribution of the total oil flow for lubrication and to cool the inner ring, appropriate radial holes and axial grooves were plugged during test bearing installation.

Test Bearings

Four bearing and cage designs were studied (figs. 2 and 3): design 1, a split-inner-ring, angular-contact ball bearing with lubrication through the inner ring, a 24° unmounted (nominal) contact angle, and an inner-ring, land-guided cage (fig. 2(a)); design 2, the same as design 1 but with a 30° unmounted contact angle; design 3, the same as design 1 but with a double-outer-ring, land-guided cage (fig. 2 (b)); design 4, a jet-lubricated, angular-contact ball bearing with relieved inner and partially relieved outer rings, a 24° unmounted contact angle, and a single-outer-ring, land-guided cage (fig. 3).

Test Procedure

After the test machine had been warmed by recirculating heated oil and the torque-measuring system had been calibrated, a 667-N (150-lbf) thrust load and a 1.9 ℓ/min (0.50-gal/min) lubricant flow rate were applied. The shaft speed was then slowly brought up to a nominal 28 000 rpm. When the bearing and test machine temperatures stabilized (after 20 to 25 min), the oil-inlet temperature and lubricant flow rate were set and the speed was increased to the desired value.

A test series was run by starting at the lowest nominal speed, 30 000 rpm, and progressing through 50 000, 65 000, and 72 000 rpm before changing the lubricant flow rate. At each speed and flow condition, a separate test was run during which the outer-ring cooling oil flow was adjusted to achieve equal inner- and outer-ring temperatures. Four lubricant flow rates ranging from 0.3 to 1.9 ℓ/min (0.08 to 0.50 gal/min) were used. The first series of tests was run with the lubrication distribution scheme shown in figure 4(a); 50 percent of the total oil flow supplied to the inner ring lubricated the bearing, 25 percent lubricated the cage lands, and 25 percent flowed axially through the bearing and cooled the inner ring. After these test runs were completed, other tests were performed to determine the effects of

(1) Adding a nominal 222-N (50-lbf) radial load to the 667-N (150-lbf) thrust load
(2) Changing the oil-flow distribution scheme to that shown in figure 4(b) in which 75 percent of the total flow supplied to the inner ring lubricated the bearing and 25 percent lubricated the cage lands with no axial oil flow through the bearing to cool the inner ring

A nominal thrust load of 667 N (150 lbf) was used for this series of tests. For each of these conditions, tests were run at nominal speeds of 50 000, 65 000, and 72 000 rpm. During testing, if it became apparent that the conditions would result in predictable distress of the test bearing or test rig or that the bearing temperature would exceed 218 °C (425 °F), the test point was aborted.

The shaft speed (inner-ring speed) was measured with a magnetic probe. The ball-pass frequency (cage speed) was measured with a semiconductor strain gage mounted in a cavity of the housing and was displayed on a spectrum analyzer.

Two thermocouples were assembled in the shaft so that the centrifugal force would push them against the test-bearing inner ring. Temperature readings were transmitted with a rotating telemetry system mounted on an auxiliary shaft at the air-turbine end of the test machine. Outer-ring temperatures were obtained by two thermocouples installed in the test-bearing housing, one located 45° from the center of the radial load zone of the bearing and the other positioned 180° from the first. For accurate measurement of oil-in and oil-out temperatures, thermocouples were placed directly in the housing fittings of the lubricating jets and in the oil discharge reservoir, as shown in figure 1.

The specifications for the test bearings are summarized in table I. The bearings were an ABEC 7 grade and each contained 16 balls with a nominal 7.14-mm (0.281-in.) diameter. The inner and outer rings and the balls were manufactured from consumable-electrode, vacuum-melted, AISI M–50 steel. The surface finishes of the races were 0.125 μm (5 μin.) rms or better. The surface finish of the balls was 0.025 μm (1 μin.). The bearing surface composite finish was 0.130 μm (5.1 μin.) The nominal hardness of the balls and rings was Rockwell C62 at room temperature.

The cage was manufactured from AISI 4340 steel (AMS 6415) heat-treated to Rockwell C 28 to 36 hardness. It was completely coated with a 0.02- to 0.04-mm (0.0008- to 0.0015-in.) thickness of silver plate (AMS 2412). The cage balance was within 0.50 g-cm (7×10^{-3} oz-in.).

The bearing design permitted lubrication through the inner ring by means of axial grooves machined in the bore. Radial holes, 0.762-mm (0.030-in.) diameter, radiating from the bearing bore formed a flow path for bearing lubrication. The bearing inner-ring grooves and radial holes were designed so that 50 percent of the oil supplied to the inner ring lubricated the bearing, 25 percent lubricated the land surfaces, and 25 percent flowed axially through those grooves that contained no radial holes. The latter flow cooled the inner ring. This oil-flow distribution is illustrated in figure 4(a). In some tests, appropriate axial grooves and radial holes were blocked to allow 75 percent of the total flow to be used for bearing lubrication, 25 percent for land surface lubrication, as shown in figure 4(b).

Lubricant

The lubricant used for the parametric studies was a neopentylpolyol (tetra) ester. This type II oil is qualified to the MIL–L–23699 specifications and also to the internal oil specifications of most major aircraft engine manufacturers. The major properties of the lubricant are presented in table II.

COMPUTER ANALYSIS

Life Analysis

The computer program SHABERTH (ref. 14) was used to calculate the contact (Hertz) stresses, contact angles, and life and thermal performance of the test bearings. The results of this analysis are summarized in table III. All computations were made with temperatures resulting from a lubricant flow rate of 0.76 ℓ/min (0.20 gal/min) with no outer-ring cooling. The measured inner- and outer-ring temperatures were used for these calculations. The effect of speed on the maximum Hertz stress and the contact angle for the inner and outer races for the nominal (unmounted) 24° and 30° contact-angle bearings is shown in figure 5. For the thrust load only, the mounted contact angles were 33° and 42°, respectively; for combined loading, the mounted contact angles were 24° and 31°, respectively. The nominal maximum Hertz stresses and contact angles under the mounted conditions are summarized in table IV.

For both nominal contact angles, the outer-race stresses increase with speed whereas the inner-race stresses remain relatively unchanged. The outer-race stress, because of centrifugal effects, exceeds that of the inner race. The bearing becomes outer-race life dependent; that is, with speed, the components that have a high probability of failure shift from the ball inner race to the ball outer race.

The outer-race contact angle decreases with speed and approaches a nearly pure radial load condition. The inner-race contact angle increases with speed. As the inner-race contact angle increases, the possibility exists for the ball-race Hertzian contact area to reach over the inner-race shoulder, an edge-loading condition that would further increase ball-race stress and could lead to premature bearing fatigue failure. This adverse condition did not occur with the designs tested.

For the thrust-load-only conditions, the inner-race contact angles were higher than those for the combined load condition. The nominal 30° contact-angle bearings had inner-race operating contact angles significantly higher than the nominal 24° contact angle. The contact angles can impact bearing heat generation whereas the resultant Hertz stress can affect bearing life.

Figure 6 shows the resultant calculations for bearing L_{10} life as a function of speed. The term L_{10} is the time in hours that 90 percent of a population of bearings would be expected to exceed without failing or that time within which 10 percent of the population will have failed. Life factors from reference 15 (table I) were incorporated in the SHABERTH computer analysis. The bearings available for testing had a composite surface finish of about 0.13 μm

(5 μin.). Composite surface finishes of 0.05 μm (2 μin.) are commonly found in better commercial quality bearings. For this analysis, it was assumed that the bearing was as manufactured and had an improved composite surface finish (σ = 0.05 μm or 2 μin.). (The composite surface finish is $\sigma = \sqrt{\sigma_b^2 + \sigma_r^2}$ where σ_b and σ_r are the rms surface finishes of the balls and races, respectively.) Also, it was assumed that the AISI M–50 steel processing was both CEVM, single vacuum melted, and VIM-VAR, double vacuum melted (table I and ref. 15). These assumptions resulted in changes to life factors a_2 for material and processing and a_3 for lubrication (ref. 15). The a_2 and a_3 life factors are summarized in tables I and III, respectively.

With reference to figure 6, life in hours decreases with speed. For thrust loading only, there is an insignificant difference in life for the nominal 24° and 30° contact-angle bearings. However, for combined loading, the 24° contact-angle bearing results in a longer life than the nominal 30° contact-angle bearing. For both bearings, the improved surface finish significantly improves bearing life. Combining this improvement in surface finish with the double-vacuum-melted (VIM-VAR) material processing of the AISI M–50 steel can further increase bearing life by an order of magnitude. Even with this life improvement, the absolute life in hours may not be sufficient for many commercial aircraft engine applications compared with what can be obtained for lower speed applications. This would imply that there is a need to further optimize bearing design for higher speed applications to obtain longer bearing life.

Thermal Analysis

The SHABERTH computer program (ref. 14) was used to calculate the bearing thermal performance. This analysis used the model system with lubricant flow paths for the split-inner-ring bearing (fig. 7). The lubricant flow paths model the experimental condition wherein half the total lubricant flow rate to the bearing passes through grooves under the inner ring and the other half is fed into the bearing cavity through a plurality of holes in the bottom of the inner-ring groove. It was assumed that the latter flow split equally to exit each side of the bearing cavity. Also, two nodes (fig. 7) were defined for each race to give a finer grid to show an axial temperature gradient in the races of the thrust-loaded bearing (ref. 16). The assumptions used in this analysis differed in some details from the lubrication scheme actually used. However, the resultant values were reasonably close to those measured.

A significant parameter required as input for bearing analysis computer programs such as SHABERTH is the percent of the bearing cavity volume that is occupied by lubricant, also called the lubricant volume percent or cavity factor XCAV. This factor describes the density of the lubricant-air mixture and is used primarily in the calculation of ball or roller drag. The bearing cavity is defined as the space between the inner and outer races that is not occupied by the cage and the balls or rollers. The authors of reference 14 recommend that the values used for XCAV be less than 5 percent. It is expected that XCAV vary with lubricant flow rate, shaft speed, and bearing size. Previous work (refs. 17 and 18) has shown that XCAV values of 2 to 3 percent generally correlate well with experimental data over a small range of conditions. Lubricant flow rate and shaft speed were not correlated with XCAV in these previous works.

Parker (ref. 16) derived an equation for XCAV based on a comparison of the heat generation, temperature, and lubricant flow rate for three sizes of angular-contact ball bearings. The Parker (ref. 16) equation for XCAV follows for SI units:

$$XCAV = 10.0 \times 10^6 \frac{W^{0.37}}{N d_m^{1.7}} \tag{1a}$$

where the variables are lubricant flow rate W, cm^3/min; inner-race speed N, rpm; and pitch diameter d_m, mm. The equation in English units is

$$XCAV = 8.62 \times 10^5 \frac{W^{0.37}}{N d_m^{1.7}} \tag{1b}$$

where W is in gal/min, N is in rpm, and d_m is in inches.

To assess the effects of shaft speed and lubricant flow on XCAV, the SHABERTH computer program was used to calculate the performance of the 35-mm-bore, angular-contact ball bearing with jet lubrication for speeds from 28 000 to 72 200 rpm and lubricant flow rates from 0.3 to 1.9 ℓ/min (0.08 to 0.50 gal/min). The thrust load and oil-in temperatures were held constant at 667 N (150 lbf) and 121 °C (250 °F), respectively. The results of this analysis are shown in figure 8. Bearing power loss increases linearly with lubricant volume percent and also increases with bearing speed. This analysis would suggest that to minimize loss at a higher speed, lubricant flow to the bearing be minimized while the temperature be maintained at acceptable levels (i.e., <218 °C (<425 °F)). The bearing (oil) temperature affects the elastohydrodynamic film thickness, which does have an effect on bearing life. Hence, the engineer must carefully balance acceptable bearing power loss and bearing life and reliability requirements. Some of the factors that influence the lubricant fill in the bearing are oil flow rate, viscosity, density, housing and shaft configuration, cage design, and bearing ring-land configuration.

Lubricant Flow Rate

A comparison of the experimental and analytical results is shown in figure 9 for bearing design 1. The measured inner- and outer-ring temperatures decreased at a decreasing rate and power consumption increased as lubricant flow rate increased. These results are consistent with other reported temperature measurements made with high-speed ball bearings.

The difference in temperature (ΔT) between the inner and outer races was mildly affected by the lubricant flow rate. At 50 000 rpm with the lower flow rate of 0.76 ℓ/min (0.20 gal/min), the ΔT between the outer and inner rings ($T_o - T_i$) was approximately 22 °C (40 °F). At 72 000 rpm, ΔT was approximately 35 °C (63 °F) with a maximum outer-race temperature of 210 °C (410 °F). As the lubricant flow rate increased to 1.9 ℓ/min (0.50 gal/min), the ΔT was reduced to 10° and 22 °C (18° and 22 °F) at 50 000 and 72 000 rpm, respectively. At 72 000 rpm, the maximum outer-race temperature was approximately 178 °C (352 °F). The results are consistent with past experience which has shown that with increased lubricant flow rate, race temperatures will decrease and then begin to increase at some intermediate flow rate.

The results of the SHABERTH computer analysis on bearing inner- and outer-ring temperatures are shown in figures 9(a) and (b). For the 50 000 rpm speed, a reasonably good correlation exists between predicted and measured temperatures with the predicted temperatures for the inner ring being about 12 °C (22 °F) less than measured. However, for the 72 000 rpm, the predicted inner-ring temperatures were approximately 16 °C less than measured. The outer-ring temperature predictions varied from 0° to approximately 16 °C (0° to 29 °F) greater than measured. If these predicted temperatures had been used to calculate the bearing internal diametral clearance (IDC) and the resultant bearing life, lower life values than those shown in figure 6 at the higher speeds would have been predicted.

So that heat rejection (power loss) could be thermally measured, oil-inlet and oil-outlet temperatures were obtained for all flow conditions. The heat absorbed by the lubricant was obtained from the standard heat-transfer equation:

$$Q_T = MC_p(t_{out} - t_{in}) \tag{2}$$

where

Q_T total heat-transfer rate to lubricant, J/min (Btu/min)

M mass flow rate, kg/min (lb/min)

C_p specific heat, J/kg K (Btu/lb °F)

t_{out} oil-outlet temperature, °C (°F)

t_{in} oil-inlet temperature, °C (°F)

Figure 9(c) shows the effect of lubricant flow rate on bearing power loss. The power loss shown was measured mechanically and thermally. The thermal measurements were consistently 0.2 kW (0.3 hp) higher than those determined mechanically. This difference can be attributed to inaccuracies in the lubricant specific heat values that were available. The mechanical measurements based on measured torque and speed were probably the more accurate of the two determinations.

The power loss increased linearly with flow rate. At a lubricant flow rate of 0.76 ℓ/min (0.20 gal/min), the power loss was approximately 0.93 kW (1.25 hp) at 50 000 rpm and 1.7 kW (2.25 hp) at 72 000 rpm. At the flow rate of 1.9 ℓ/min (0.50 gal/min), the power loss was 1.4 kW (1.9 hp) at 50 000 rpm and 1.6 and 3.2 kW (2.2 and 4.3 hp) at 50 000 and 72 000 rpm, respectively.

The predicted power loss (fig. 9(c)) showed the same trend as the experimental data but was less than that measured mechanically or thermally. The differences between the measured and predicted losses were reasonably consistent. At 50 000 rpm, the difference between the power loss measured thermally and that calculated ranged from 0.4 to 0.8 kW (0.5 to 1.1 hp). At 70 000 rpm, this difference was approximately 0.8 kW (1.1 hp).

Effect of Speed

The effect of speed on bearing temperature and power loss was studied for design 1 (fig, 2(a)) under a thrust load of 667 N (150 lbf). Speed was varied from 31 000 to 72 000 rpm. The oil-in temperature was 121 °C (250 °F). As expected, when the speed was increased, the temperature for the inner and outer rings increased and varied from approximately 135 °C (275 °F) for both rings at the lower speed to approximately 155 °C (311 °F) for the inner ring and 181 °C (358 °F) for the outer ring at 72 000 rpm (fig. 10(a)). The difference between the outer- and inner-ring ($T_o - T_i$) temperatures (ΔT) varied from 0° to 26 °C (0° to 47 °F). The resultant Hertz stresses as a function of speed and contact angle are summarized in tables III and IV and in figure 5.

In addition to the 667-N (150-lbf) thrust load, a radial load of 222 N (50 lbf) was applied to the bearing. This resulted in a nominal maximum Hertz stress of 1.7 and 1.3 GPa (247 and 189 ksi) on the inner and outer races, respectively (table IV). The inner-ring temperature rose less than 5 °C (9 °F) and the outer-ring temperature decreased by similar amounts at each speed (fig. 10(a)).

It is desirable to thermally manage the bearing so that the internal diametral clearance (IDC) in the bearing remains within a narrow range. As speed is increased and as the ΔT across the bearing increases, IDC increases. This increase in the IDC results in increased contact stresses for a given bearing load, causing a decrease in bearing life. A way to control IDC is by cooling the bearing outer raceway. This method was extensively reported by Zaretsky, Bamberger, and Signer (refs. 1 to 4). Figure 10(b) shows the effect of bearing outer-ring cooling on inner- and outer-ring temperatures. In these tests, the outer-ring cooling was used to match the inner- and outer-ring temperatures. In some cases, as in those shown in figure 10(c), the inner- and outer-ring temperatures were nearly the same without the use of outer-ring cooling.

Figure 10(c) shows the effect of speed on power loss for the bearing with and without outer-ring cooling and with a combined load and with a thrust load only. As would be expected, power loss increases with speed and load. The power loss ranged from approximately 0.5 kW (0.7 hp) at 30 000 rpm for a thrust load only to approximately 2.6 kW (3.5 hp) at 72 000 rpm. Outer-ring cooling had only a nominal effect on bearing power loss. The combined load on the bearing increased the power loss by less than 0.4 kW (0.5 hp).

In figure 10, the experimental results were compared with the SHABERTH computer code predictions for race temperatures and power loss as a function of speed. For outer-ring temperatures without outer-ring cooling, the predicted race temperature was approximately 20 °C (36 °F) lower than that measured at 31 000 rpm and was approximately 15 °C (27 °F) higher than that measured at 72 000 rpm. At approximately 50 000 rpm, the predicted and measured outer-ring temperatures were approximately equal. For the inner ring temperatures, the predicted temperatures were 10° to 15 °C (18° to 27 °F) lower than those measured. There is a reasonably good engineering correlation between the predicted and measured temperature ranges.

As previously discussed, the stress and life calculations are in part dependent on the value of ΔT. When no outer-ring cooling was provided (fig. 9(a)), the experimental measurements and the prediction show a ΔT of approximately zero at 31 000 rpm. For the life and stress calculations of table III and figures 5 and 6, the actual measured race temperatures were used. If the calculated values of ΔT were used, the resultant stresses would be higher and the calculated life lower than those shown.

Optimal operating conditions for this bearing at high speed can be achieved by using outer-ring cooling in conjunction with low lubricant flow rates. This results in a power loss reduction of approximately 40 percent.

Effect of Contact Angle

As the bearing contact angle is increased, the load capacity of a bearing and thus the life are expected to increase for a predominately thrust-loaded bearing. Common wisdom would dictate that as bearing contact angle is increased, the internal heat generation in the bearing and resulting power loss would also increase. A general rule for most turbomachinery applications is that the nominal contact angle of a bearing is restricted to less than 25° to minimize heat generation. In the application, as a static thrust load is applied to a bearing, the operating contact angle is increased. The actual operating contact angle of a bearing under combined loading varies around the bearing. As bearing speed increases beyond 1M DN, the operating contact angle increases with speed on the inner race and decreases on the outer race. Ball spinning and thus heat generation changes with contact angle. It is generally expected that with higher contact angles there will be greater ball spinning and hence higher heat generation and race temperatures for a constant lubricant flow rate. However, for most rolling-element bearings, the major source of heat generation is caused by the volume of lubricant trapped within the bearing cavity where it is churned, plowed, and sheared by the action of the rolling elements and the cage.

For bearing design 1, the temperature and heat generation were expected to be lower than those for bearing design 2. The effect of contact angle on bearing temperature and power loss is shown in figure 11. The race temperatures of the 30° contact-angle bearing were on the order of 2° to 4 °C (3.6° to 7.2°F) less than those of the 24° contact-angle bearing. This difference in temperature is not considered significant. The power loss for the 24° contact-angle bearing was slightly less than that for the 30° contact bearing. The power difference was less than 0.2 kW (0.3 hp) over the range of speeds, which is not significant for these data.

These data would suggest that as the contact angle is increased, the decrease in the ball normal load and the decrease in the major axis of the contact ellipse offset the effect of increased spin velocity on heat generation.

Cage Design

For decades, the issue of whether a bearing should be designed with an inner- or an outer-ring, land-guided cage has been vigorously discussed by designers of turbomachinery and rolling-element bearings. Over the years, high-speed bearings have been designed and operated successfully with both types of cages. However, there is a limited data base comparing these cage designs under identical conditions of operation and in the same test facility.

The split-inner-ring, 35-mm bore, angular-contact ball bearing used in this investigation was designed to accommodate either an inner- or outer-ring, land-guided cage. These designs are shown in figure 2. Tests were conducted with bearing designs 1 and 3 (fig. 2) and bearing design 4 (fig. 3). Bearing design 4 was conceived to optimize oil flow into and out of the bearing. The results of these tests are shown in figure 12. The inner-ring temperatures as a function of speed were nearly identical for the three bearing designs. However, the outer-ring temperatures were significantly different and were a function of cage design and location. The highest temperatures and power loss occurred for the split-inner-ring bearing with a double-outer-ring, land-guided cage. The outer-ring temperatures ranged from approximately 176° to 217 °C (349° to 425 °F) and the power loss ranged from 1.2 to 2.1 kW (1.6 to 2.8 hp). For the split-inner-ring bearing with the inner-ring, land-guided cage, the outer-ring temperatures and power loss were lower. The outer-ring temperatures were approximately 10 °C (18 °F) lower for the bearing with the single-outer-ring, land-guided cage than that for the bearing with the double-outer-ring, land-guided cage. The power loss was approximately 0.5 kW (0.7 hp) less.

The single-outer-ring, land-guided cage provided the lowest outer-ring temperatures and power loss. The outer-ring temperatures were approximately 20° to 35 °C (36° to 51 °F) lower than those for the double-outer-ring, land-guided cage with the split-inner-ring bearing. The power loss was approximately 0.7 to 1.3 kW (0.9 to 1.7 hp). In previously reported tests (refs. 6 and 8), equivalent bearings with a jet-lubricated, single-outer-ring, land-guided cage also resulted in the lowest temperatures and power loss when compared with bearings with a jet-lubricated, double-outer-ring, land-guided cage and an inner-ring-lubricated, single-outer-ring, land-guided cage. The probable reason for the lower temperatures and power loss for the single-outer-ring, land-guided cage with a partially relieved outer ring is that more oil is evacuated from the bearing with minimum churning. This would suggest that the Parker formula (eqs. (1a) and (b)) for XCAV may need to be refined to reflect bearing lubrication mode, cage design and location, and internal geometry modifications.

SUMMARY OF RESULTS

The computer program SHABERTH was used to analyze a 35-mm-bore, angular-contact ball bearing designed and manufactured for high-speed turbomachinery applications. Parametric tests of the bearing were conducted in a high-speed, high-temperature bearing tester. Four bearing and cage designs were studied (figs. 2 and 3). The test conditions were shaft speeds from 28 000 to 72 000 rpm (1 to 2.5 M DN, the speed of the shaft in revolutions per minute multiplied by the bearing bore in millimeters) and an oil-inlet temperature of 121 °C (250 °F). Both jet and under-ring lubrication were studied. Outer-ring cooling was provided in some tests. The lubricant was a neopentylpolyol (tetra) ester that met the MIL–L–23699 specification. The following results were obtained:

1. The predicted bearing life decreased with increasing speed because of increased operating contact stresses due to changes in contact angle and centrifugal load. For thrust loads only, the difference in calculated life for the nominal 24° and 30° contact-angle bearings was insignificant. However, for combined loading, the 24° contact-angle bearing gave longer life.

2. For split-inner-ring bearings, optimal operating conditions were obtained with a 24° contact angle and an inner-ring, land-guided cage using outer-ring cooling in conjunction with low lubricant flow rates.

3. Lower temperature and power losses were obtained with a single-outer-ring, land-guided cage for the 24° contact-angle bearing having a relieved inner ring and a partially relieved outer ring.

4. Inner-ring temperatures were independent of lubricant mode and cage design.

5. Reasonably good engineering correlation was obtained using the computer program SHABERTH for predicted bearing power loss and predicted inner- and outer-ring temperatures in comparison with measured values. The Parker formula for XCAV (in SHABERTH, a measure of oil volume in the bearing cavity) may need to be refined to reflect bearing lubrication mode, cage design, and location of the cage controlling land.

REFERENCES

1. Zaretsky, E.V.; Bamberger, E.N.; Signer, H.: Operating Characteristics of 120-Millimeter-Bore Ball Bearings at 3×10^6 DN. NASA TN D–7837, 1974.
2. Signer, H.; Bamberger, E.N.; and Zaretsky, E.V.: Parametric Study of the Lubrication of Thrust Loaded 120-mm-Bore Ball Bearings to 3 Million DN. J. Lubr. Tech., Trans. ASME, vol. 96, no. 3, July 1974, pp. 515–525.
3. Bamberger, E.N.; Zaretsky, E.V.; and Signer, H.: Effect of Speed and Load on Ultra-High-Speed Ball Bearings. NASA TN D–7870, 1975.
4. Bamberger, E.N.; Zaretsky, E.V.; and Signer, H.: Endurance and Failure Characteristic of Main-Shaft Jet Engine Bearing at 3×10^6 DN. J. Lubr., Tech. Trans. ASME, vol. 98, no. 4, Oct. 1976, pp. 580–585.
5. Schuller, F.T.; Pinel, S.I.; and Signer, H.R.: Operating Characteristics of High-Speed, Jet-Lubricated 35-Millimeter-Bore Ball Bearing With a Single-Outer-Land-Guided Cage. NASA TP–1657, 1980.
6. Schuller, F.T.; Pinel, S.I.; and Signer, H.R.: Effect of Cage Design on Characteristics of High-Speed-Jet-Lubricated 35-Millimeter-Bore Ball Bearings. NASA TP–1732, 1980.
7. Schuller, F.T.; and Signer, H.R.: Performance of Jet- and Inner-Ring-Lubricated 35-Millimeter-Bore Ball Bearings Operating to 2.5 Million DN. NASA TP–1808, 1981.
8. Signer, H.R.; and Schuller, F.T.: Lubrication of 35-Millimeter-Bore Ball Bearings of Several Designs at Speeds to 2.5 Million DN. Problems in Bearings and Lubrication, AGARD CP–320, 1983.
9. Schuller, F.T.: Lubrication of 35-Millimeter-Bore Ball Bearings of Several Designs to 2.5 Million DN. Advanced Power Trans. Tech., Fischer, G.K. ed., NASA CP–2210, pp. 221–237, 1983.
10. Schuller, F.T.; Pinel, S.I.; and Signer, H.R.: Effect of Two Inner-Ring Oil-Flow Distribution Schemes on the Operating Characteristics of a 35-Millimeter-Bore Ball Bearing to 2.5 Million DN. NASA TP–2404, 1985.
11. Zaretsky, E.V.; Schuller, F.T.; and Coe, H.H.: Lubrication and Performance of High-Speed Rolling-Element Bearings. Lubrication Engr., vol. 41, no. 12, Dec. 1985, pp. 725–732.
12. Pinel, S.I.; and Signer, H.R.: Development of a High-Speed, Small Bore Bearing Test Machine. NASA CR–135083, 1976.
13. Miyakawa, Y.; Seki, K.; and Yokoyama, M.: Study on the Performance of Ball Bearings at High DN Values. NASA TT F–15017, translation of Koh DN Chi Ni Okeru Gyokujikuju No Seino Ni Kansuru Kenkyu, National Aerospace Lab., Tokyo, Japan, Report NAL–TRL–284, 1973.

14. Hadden, G.B., et al.: Research Report: User's Manual for Computer Program AT81Y003 SHABERTH. Steady State and Transient Thermal Analysis of a Shaft Bearing System Including Ball, Cylindrical, and Tapered Roller Bearings. NASA CR–165365, 1981.
15. Zaretsky, E.V., ed.: STLE Life Factors for Rolling Bearings. STLE, Park Ridge, IL, SP–34, 1992.
16. Parker, R.J.: Comparison of Predicted and Experimental Thermal Performance of Angular-Contact Ball Bearings. NASA TP–2275, 1984.
17. Coe, H.H.; and Zaretsky, E.V.: Predicted and Experimental Performance of Jet-Lubricated 120-Millimeter-Bore Ball Bearings Operating to 2.5 Million DN. NASA TP–1196, 1978.
18. Coe, H.H.; and Schuller, F.T.: Comparison of Predicted and Experimental Performance of Large-Bore Roller Bearing Operating to 3.0 Million DN. NASA TP–1599, 1980.

TABLE I.—TEST BEARING SPECIFICATIONS

Bearing	
Bore, mm (in.)	35 (1.3780)
Outside diameter, mm (in.)	62 (2.4409)
Width, mm (in.)	14 (0.5512)
Grade	ABEC 7
Surface composite finish, μm (μin.)	0.130 (5.1)
Cage	
Diametral land clearance, mm (in.)	
Outer-land-guided	0.406 (0.016)
Inner-land-guided	0.254 (0.010)
Diametral ball pocket clearance, mm (in.)	0.660 (0.026)
Material	AISI 4340 per AMS 6415 (silver plated)
Hardness, Rockwell C	32 to 38
Balls	
Number	16
Size (diam), mm (in.)	7.14 (0.281)
Grade	10
Material	CEVM AISI M–50 per AMS 6490
Hardness, Rockwell C (nominal)	62 (min.)
Surface finish, μm (μin.) rms	0.025 (1)
Race	
Conformity, percent	
Inner	54
Outer	52
Surface finish, μm (μin.), rms	0.125 (5)
Nominal contact angle, deg	24 or 30
Internal diametral clearance (IDC), μm (μin.)	
Split inner ring	
24° contact angle	0.061 (0.0024)
30° contact angle	0.102 (0.0040)
Angular-contact ball bearing, relieved inner race	
24° contact angle	0.074 (0.0029)
STLE life factors (from ref. 15)	
For material, a_2	
AISI M–50	2
Processing	
CEVM	3
VIM-VAR	6
For lubrication, a_3	(see Table 3)

TABLE II.—PROPERTIES OF NEOPENTYLPOLYOL (TETRA) ESTER LUBRICANT

Additives	
Corrosion and oxidation inhibitors and antiwear and antifoam additives	
Kinematic viscosity, cS, at—	
38 °C (100 °F)	28.5
99 °C (210 °F)	5.22
204 °C (400 °F)	1.31
Flashpoint, °C (°F)	260 (500)
Autogenous ignition temperature, °C (°F)	421 (800)
Pour point, °C (°F)	-59 (-75)
Volatility (6.5 hr at 204 °C (400 °F)), wt%	3.2
Specific heat at 99 °C (210 °F), J/kg·°C (Btu/lb·°F)	2140 (0.493)
Thermal conductivity at 204 °C (400°F), J/m·sec·°C (Btu/hr·ft·°F)	0.13 (0.075)
Specific gravity at 99 °C (210 °F)	0.931
Specification	MIL–L–23699

TABLE III.—SUMMARY OF COMPUTER ANALYSIS OF SPLIT-INNER-RING, 35-mm-BORE, ANGULAR-CONTACT BALL BEARING

[Steel, AISI M–50; material processing, CEVM or VIM-VAR; thrust load, 667 N (150 lbf); radial load, 222 N (50 lbf); nominal contact angle, 24° or 30°, type of lubrication, under race; outer-ring cooling, none; cage, inner-ring-guided; lubricant, neopentylpolyol (tetra) ester; oil-in temperature, 121 °C (250 °F); lubricant flow rate, 0.76 ℓ/min (0.20 gal/min).]

Speed, rpm		Maximum Hertz stress, GPa (ksi)		Contact angle, deg		Lubrication life factor, a_3				Bearing life, L_{10}, hr			
Inner race	Cage (epicyclic)	Inner race	Outer race	Inner race	Outer race	Composite surface finish, σ = 0.13 μm (5 μin.)		Composite surface finish, σ = 0.05 μm (2 μin.)		Life factor for material and processing, a_2 = 6		Life factor for material and processing, a_2 = 12	
						Inner race	Outer race	Inner race	Outer race	Composite surface finish, σ = 0.13 μm (5 μin.)	Composite surface finish, σ = 0.05 μm (2 μin.)	Composite surface finish, σ = 0.13 μm (5 μin.)	Composite surface finish, σ = 0.05 μm (2 μin.)
24° contact angle with thrust load only													
50×10^3	24.1×10^3	1.22 (177)	1.54 (223)	40.2	8.4	1.36	0.94	2.54	2.46	2856	14 652	5712	29 304
65×10^3	33.1×10^3	1.22 (177)	1.80 (261)	39.6	5.2	1.27	.53	2.49	2.20	316	2715	632	5430
72×10^3	35×10^3	1.23 (178)	1.91 (277)	38.5	4.4	1.07	.43	2.49	2.20	133	1361	266	2722
24° contact angle with combined load													
50×10^3	24.3×10^3	1.53 (222)	1.60 (232)	26.3	10.3	1.09	0.66	2.49	2.36	1750	12 020	3500	24 040
65×10^3	31.6×10^3	1.54 (223)	1.88 (273)	26.1	6.1	.93	.45	2.45	2.23	250	2443	500	4886
72×10^3	35.1×10^3	1.55 (225)	2.00 (290)	25.9	5.1	.85	.35	2.43	2.10	102	1213	204	2426
30° contact angle with thrust load only													
50×10^3	26.5×10^3	1.14 (165)	1.60 (232)	51.4	7.5	1.42	1.10	2.55	2.49	2383	10 660	4766	21 320
65×10^3	34.8×10^3	1.14 (165)	1.89 (274)	51.1	4.5	1.28	.92	2.53	2.45	335	1864	670	3728
72×10^3	39.4×10^3	1.14 (165)	2.04 (296)	51.0	3.6	1.35	.70	2.54	2.38	126	812	252	1624
30° contact angle with combined load													
50×10^3	27.0×10^3	1.50 (218)	1.74 (252)	32.5	8.5	1.37	0.85	2.54	2.43	1450	8163	2900	16326
65×10^3	35.3×10^3	1.51 (219)	2.09 (303)	33.1	5.6	1.22	0.55	2.52	2.30	169	1407	338	2814
72×10^3	39.9×10^3	1.52 (220)	2.24 (325)	33.6	4.5	1.56	0.46	2.57	2.23	63	602	126	1204

TABLE IV.—SUMMARY OF STATIC MAXIMUM HERTZ STRESS UNDER MOUNTED CONDITONS FOR SPLIT-INNER-RING, 35-mm-BORE, ANGULAR-CONTACT BALL BEARING

[Steel, AISI M–50; material processing, CEVM or VIM-VAR; thrust load, 667 N (150 lbf); radial load, 222 N (50 lbf); inner-race conformity, 54 percent; outer-race conformity, 52 percent.]

Contact angle, deg		Type of load	Maximum Hertz stress, Gpa (ksi)	
Nominal	Mounted and with test load		Inner race	Outer race
24	33.0	Thrust load only	1.3 (189)	1.0 (145)
	24.5	Combined load	1.7 (247)	1.3 (189)
30	41.7	Thrust load only	1.2 (174)	.9 (131)
	30.9	Combined load	1.7 (247)	1.3 (189)

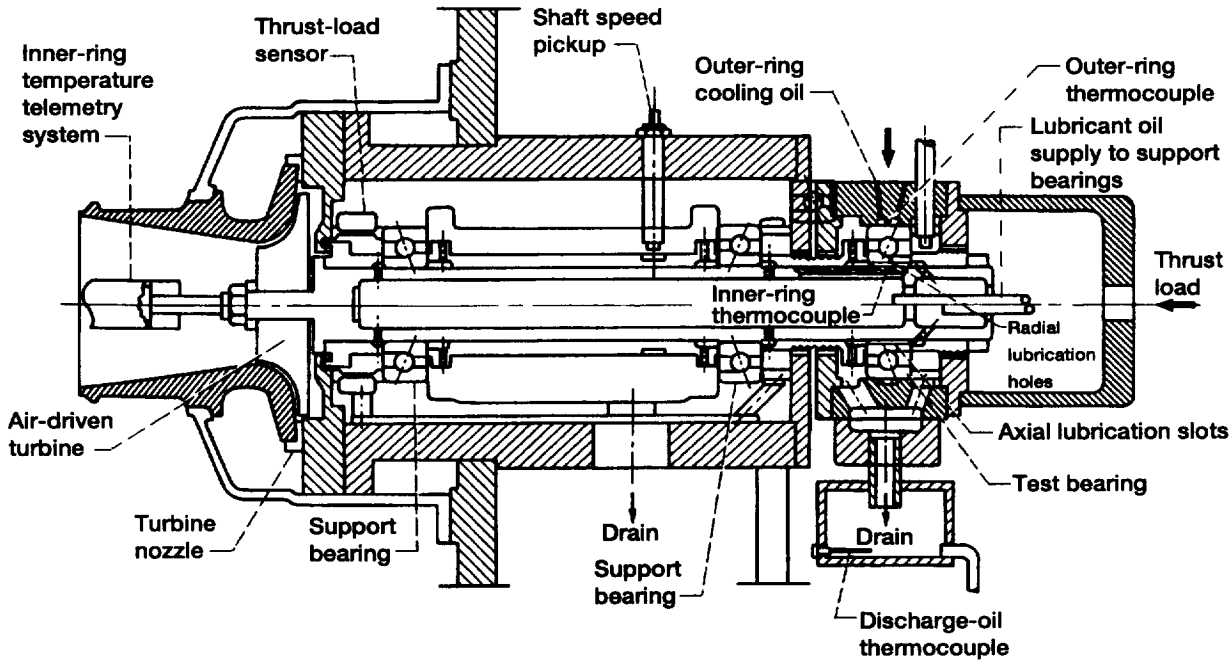

Figure 1.—High-speed, small-bore-bearing tester.

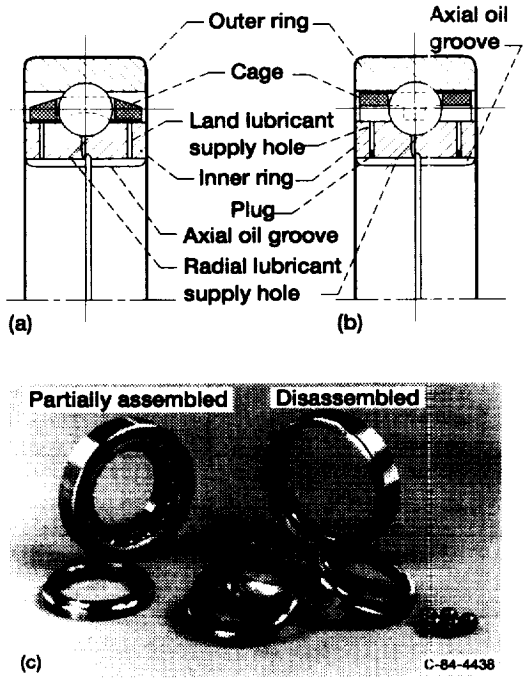

Figure 2.—Split-inner-ring, 35-mm-bore, angular-contact ball bearing. (a) Double inner-ring, land-guided cage (designs 1 and 2). (b) Double outer-ring, land-guided cage (design 3). (c) Bearing assembly.

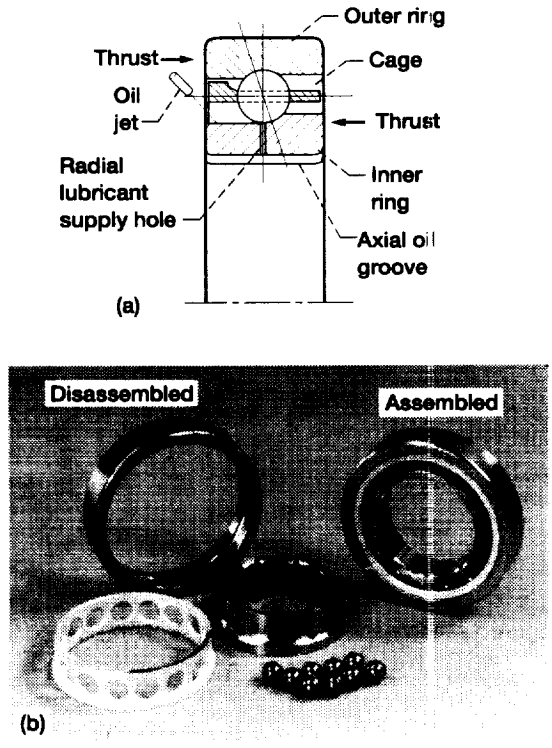

Figure 3.—35-mm-bore, angular-contact ball bearing with relieved inner ring (design 4). (a) Single outer-ring, land-guided cage. (b) Bearing assembly.

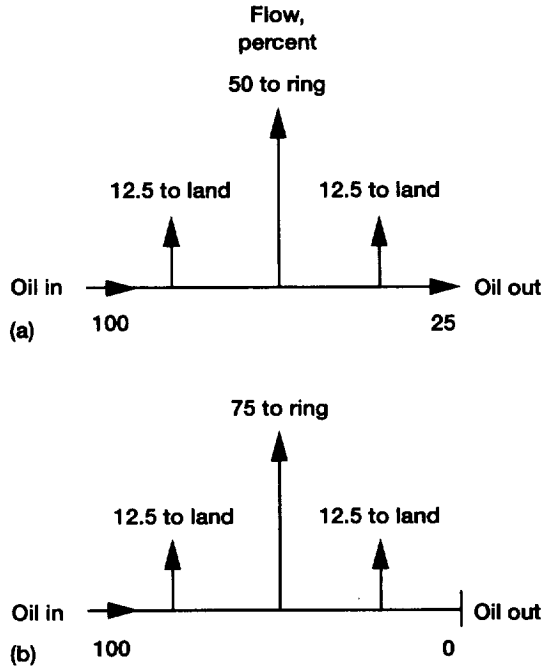

Figure 4.—Oil-flow distribution through inner ring. (a) 50 percent flow. (b) 75 percent flow.

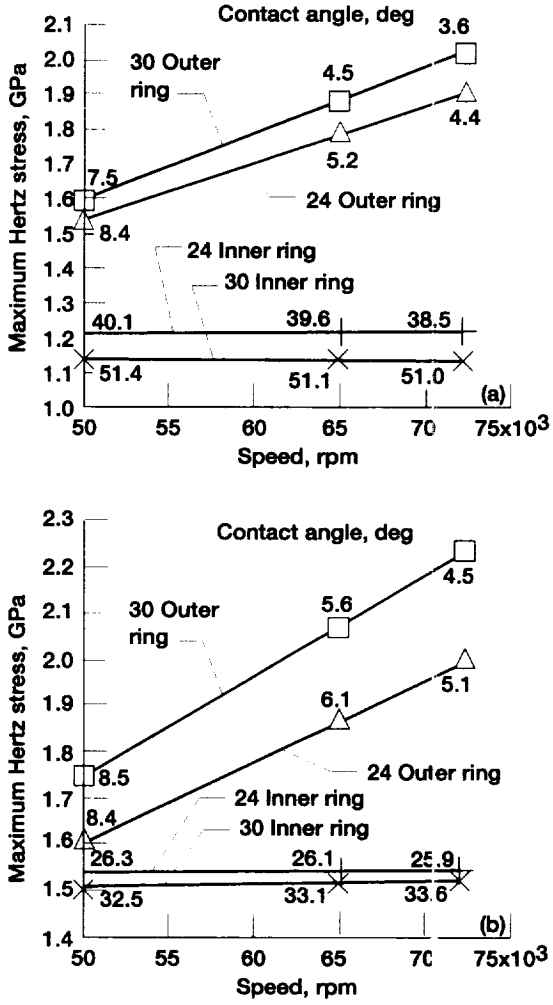

Figure 5.—Effect of speed on maximum Hertz stress and contact angle for 35-mm-bore, angular-contact ball bearing. Inner-race conformity, 54 percent; outer-race conformity, 52 percent; nominal (unmounted) contact angle, 24° or 30°. (a) Thrust load, 667 N (150 lbf); radial load, none. (b) Thrust load, 667 N (150 lbf); radial load, 222 N (50 lbf).

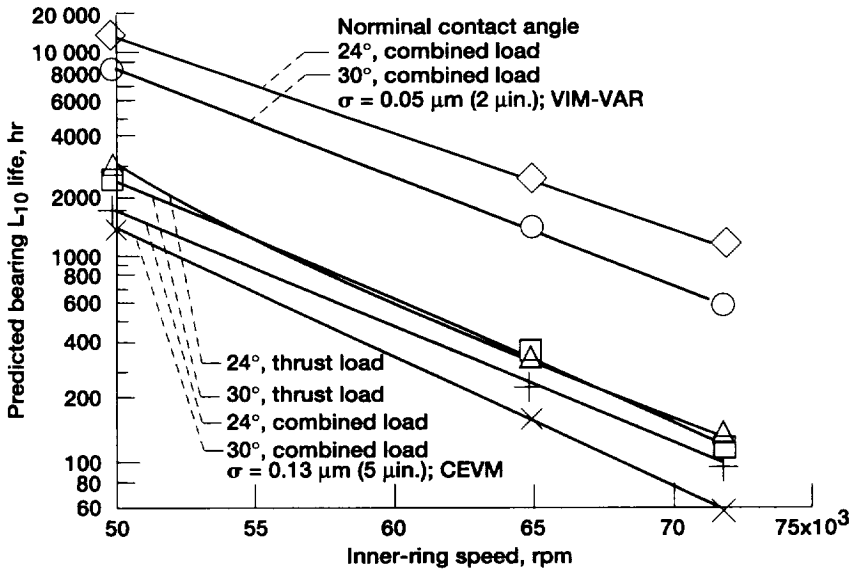

Figure 6.—Predicted bearing L_{10} life of split-inner-ring, AISI M–50 steel, 35-mm-bore, angular-contact ball bearing (based on measured ring temperatures without outer-ring cooling) as function of speed, material processing, contact angle, and surface finish, σ.

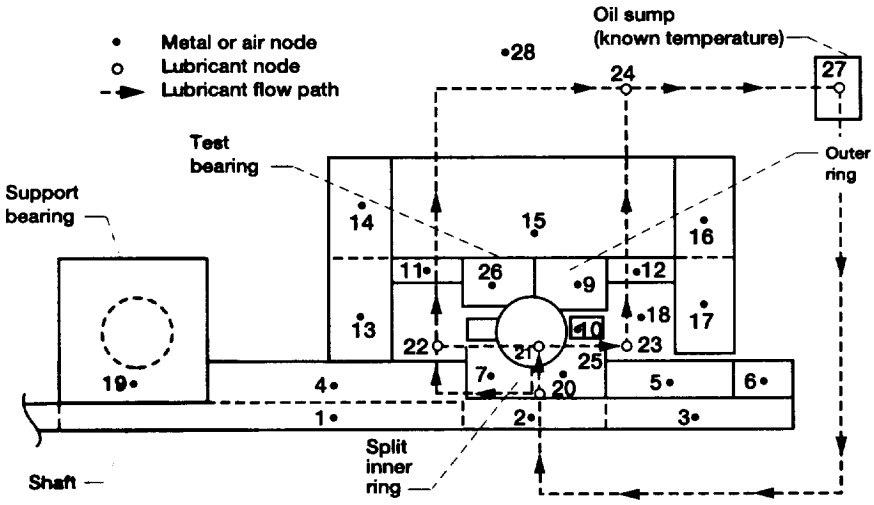

Figure 7.—Nodal system and lubricant flow paths used to model 35-mm-bore ball bearing tests with through-the-ring lubrication (from ref. 16).

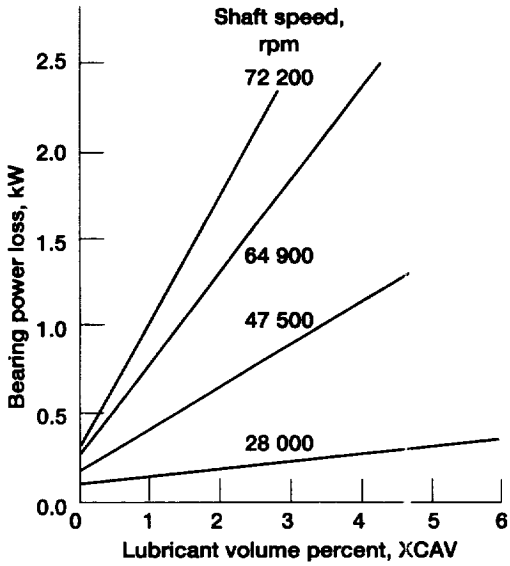

Figure 8.—Effect of lubricant volume percent (XCAV) on bearing power loss calculated by SHABERTH computer program. Bearing type, 35-mm-bore, angiar-contact ball; thrust load, 667 N (150 lbf); contact angle, 24°; type of lubrication, jet; oil-inlet temperature, 121 °C (250 °F); lubricant, neopentylpolyol (tetra) ester (Mil–L–23699) (ref. 16).

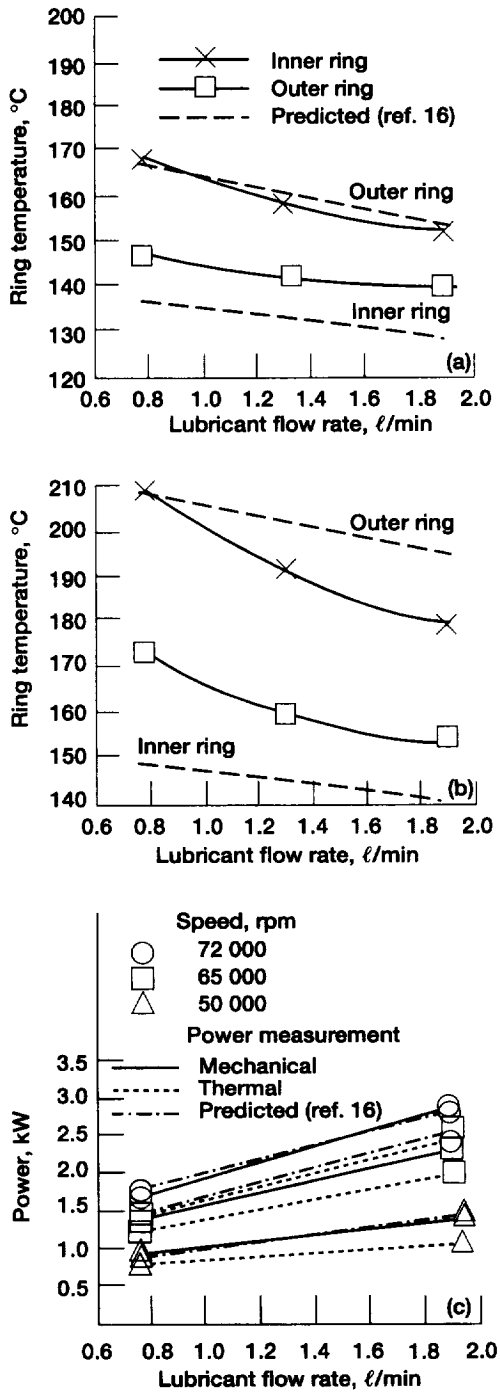

Figure 9.—Effect of lubricant flow rate on bearing temperature and power loss of split-inner-ring, 35-mm-bore, angular-contact ball bearing (design 1, fig. 2 (a)). Thrust load, 667 N (150 lbf); normal contact angle 24°; cage, inner-ring, land-guided; type of lubrication, flow through split inner ring. (a) Ring temperature for 50 000 rpm. (b) Ring temperature for 72 000 rpm. (c) Power loss.

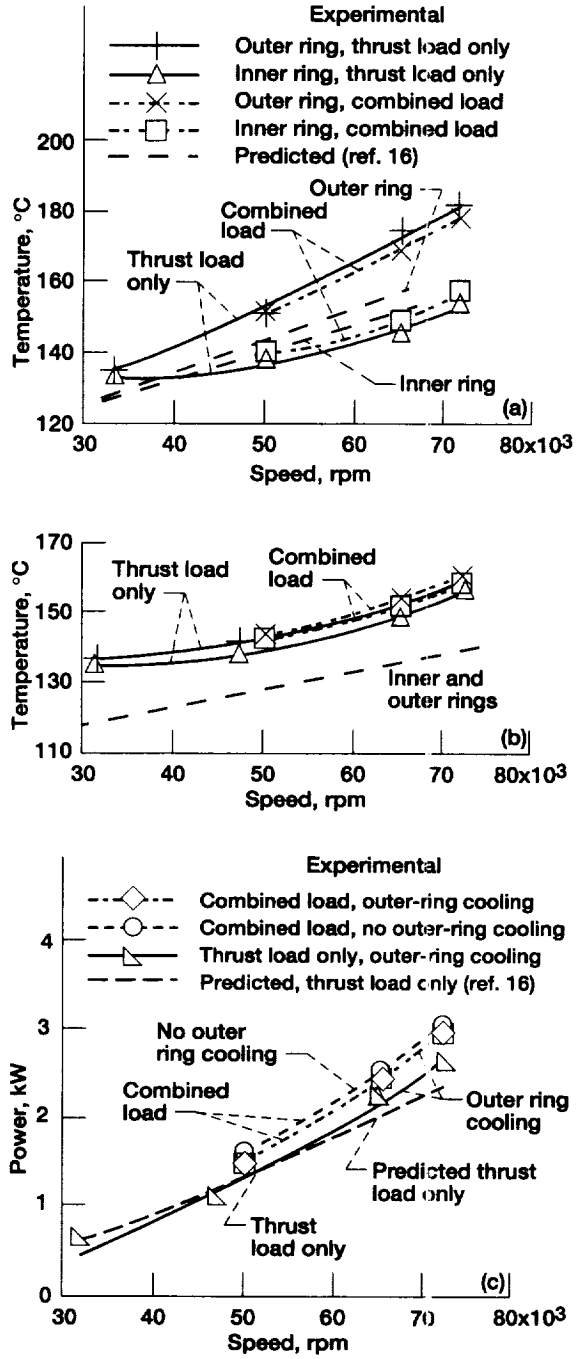

Figure 10.—Effect of speed on bearing temperature and power loss of split-inner-ring, 35-mm-bore, angular-contact ball bearing (design 1, fig. 2 (a)). Thrust load, 667 N (150 lbf); radial load, 222 N (50 lbf); nominal contact angle, 24°; cage, inner-ring, land-guided; type of lubrication, flow through split inner ring. (a) Ring temperature with no outer-ring cooling. (b) Ring temperature with outer-ring cooling. (c) Power loss.

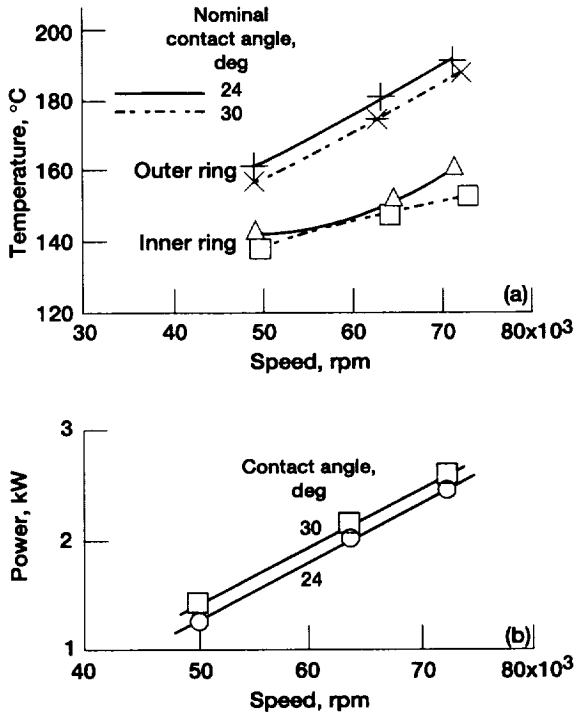

Figure 11.—Effect of contact angle on temperature and power loss for split-inner-ring, 35-mm-bore, angular-contact ball bearing (designs 1 and 2, fig. 2 (a)). Thrust load, 667 N (150 lbf); radial load, 222 N (50 lbf); type of lubrication, flow through split inner ring; lubricant flow rate, 1.32 ℓ/min (0.35 gal/min); cage, inner-ring, land-guided. (a) Temperature. (b) Power loss.

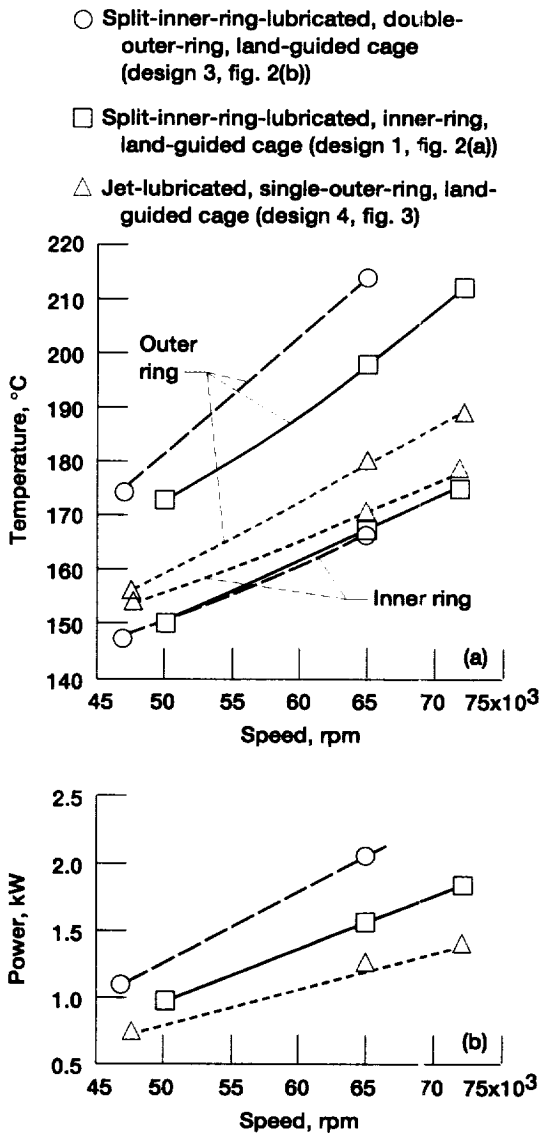

Figure 12.—Effect of cage design on temperature and power loss for 35-mm-bore, angular-contact ball bearing. Thrust load, 667 N (150 lbf); radial load, 222 N (50 lbf); nominal contact angle, 24°; lubricant flow rate, 0.76 ℓ/min (0.20 gal/min); outer-ring cooling, none. (a) Temperature. (b) Power loss.

REPORT DOCUMENTATION PAGE

Form Approved
OMB No. 0704-0188

1. AGENCY USE ONLY (*Leave blank*)	2. REPORT DATE	3. REPORT TYPE AND DATES COVERED
	August 1998	Technical Memorandum

4. TITLE AND SUBTITLE

Design and Operating Characteristics of High-Speed, Small Bore, Angular-Contact Ball Bearings

5. FUNDING NUMBERS

WU-523-22-13-00

6. AUTHOR(S)

Stanley I. Pinel, Hans R. Signer, and Erwin V. Zaretsky

7. PERFORMING ORGANIZATION NAME(S) AND ADDRESS(ES)

National Aeronautics and Space Administration
Lewis Research Center
Cleveland, Ohio 44135-3191

8. PERFORMING ORGANIZATION REPORT NUMBER

E-10702

9. SPONSORING/MONITORING AGENCY NAME(S) AND ADDRESS(ES)

National Aeronautics and Space Administration
Washington, DC 20546-0001

10. SPONSORING/MONITORING AGENCY REPORT NUMBER

NASA TM—1998-206981

11. SUPPLEMENTARY NOTES

Prepared for the Annual Meeting sponsored by the Society of Tribologists and Lubrication Engineers, Detroit, Michigan, May 17–22, 1998. Stanley I. Pinel, Pinel Engineering, Placentia, California; Hans R. Signer, Signer Technical Services, Fullerton, California; and Erwin V. Zaretsky, NASA Lewis Research Center. Responsible person, Erwin V. Zaretsky, organization code 5900, (216) 433–3241.

12a. DISTRIBUTION/AVAILABILITY STATEMENT

Unclassified - Unlimited
Subject Category: 37 Distribution: Nonstandard

This publication is available from the NASA Center for AeroSpace Information, (301) 621–0390.

12b. DISTRIBUTION CODE

13. ABSTRACT (***Maximum 200 words***)

The computer program SHABERTH was used to analyze 35-mm-bore, angular-contact ball bearings designed and manufactured for high-speed turbomachinery applications. Parametric tests of the bearings were conducted on a high-speed, high-temperature bearing tester and were compared with the computer predictions. Four bearing and cage designs were studied. The bearings were lubricated either by jet lubrication or through the split inner ring with and without outer-ring cooling. The predicted bearing life decreased with increasing speed because of increased operating contact stresses caused by changes in contact angle and centrifugal load. For thrust loads only, the difference in calculated life for the 24° and 30° contact-angle bearings was insignificant. However, for combined loading, the 24° contact-angle bearing gave longer life. For split-inner-ring bearings, optimal operating conditions were obtained with a 24° contact angle and an inner-ring, land-guided cage, using outer-ring cooling in conjunction with low lubricant flow rates. Lower temperature and power losses were obtained with a single-outer-ring, land-guided cage for the 24° contact-angle bearing having a relieved inner ring and partially relieved outer ring. Inner-ring temperatures were independent of lubrication mode and cage design. In comparison with measured values, reasonably good engineering correlation was obtained using the computer program SHABERTH for predicted bearing power loss and for inner- and outer-ring temperatures. The Parker formula for XCAV (used in SHABERTH, a measure of oil volume in the bearing cavity) may need to be refined to reflect bearing lubrication mode, cage design, and location of cage-controlling land.

14. SUBJECT TERMS

Ball bearings; High-speed turbomachinery; Bearing life and reliability

15. NUMBER OF PAGES

28

16. PRICE CODE

A03

17. SECURITY CLASSIFICATION OF REPORT	18. SECURITY CLASSIFICATION OF THIS PAGE	19. SECURITY CLASSIFICATION OF ABSTRACT	20. LIMITATION OF ABSTRACT
Unclassified	Unclassified	Unclassified	